Al-Salam Journal for Engineering and Technology
Journal Homepage: http://journal.alsalam.edu.iq/index.php/ajest
e-ISSN: 2790-4822 p-ISSN: 2958-0862

Numerical Investigation on Improving The Effectiveness of Film Cooling Using Vortex Generators

Karrar E. Finjan[1]*, Ammar F. Abdulwahid[1]

[1]Department of Mechanical, College of Engineering, University of Kufa, Iraq.

*Corresponding Author: Karrar E. Finjan

DOI: https://doi.org/10.55145/ajest.2025.04.01.006
Received June 2024; Accepted August 2024; Available online August 2024

ABSTRACT: Film cooling is an effective way for the blades to cool of an exceptionally powerful gas turbine. This process involves injecting a cooler fluid, typically air. The injected fluid forms a thin insulating layer or "film" that protecting the underlying material from thermal damage. However, due to the primary flow and film jet's interaction, a counter-rotating vortex pair is created, which causes severe jet-off and inadequate film coverage. Protrusion V-shaped and rectangular winglet vortex generators were employed In this research at the top place of the film hole to impede the counter-rotating vortex pair, in an effort to boost cooling's efficiency. Numerical simulations with Realizable k-ε were solved at a blowing ratio was between 0.5–2 and a 30° inclination angle. Results shows that vortex generators of both kinds can produce more anti-counter-rotating vortex pairs to be able to lessen the strength of the counter-rotating vortex pairs. The downwash vortices produced by the vortex generators lessen the detrimental effects of the counter-rotating vortex pair. Downwash vortices and counter-rotating vortex pair are engaged in a competitive mechanism, hence as the ratio of blowing rises, the vortex generators' favorable effects will diminish. So it was noted through this study that the best blowing ratio is (1.0). When the blowing ratio is 1.0, the results demonstrate improved film cooling performance for the flat plate. This was observed for both types of vortex generators. Specifically, the rectangular vortex generator showed this capability, with the average effectiveness of adiabatic film cooling surpassing the baseline case by 27.33%.

Keywords: Film cooling, Vortex generators, Jet-in-cross-flow

1. INTRODUCTION

Gas temperature upstream the advanced aero engines' turbine inlet has surpassed 2000 K [1]. The sliding of crystals within metallic materials causes the creep phenomenon when they are exposed to heat loads and high temperatures over an extended period of time. Metal material can fracture via creep as a result of increased centrifugal forces when operating at a fast speed [2]. Furthermore, liquid particles from insufficient burning may be deposited on high-temperature blades, obstructing the blades' hollow interior [3]. Aero-engine turbine blades widely use film cooling technology as an effective cooling technique [4]. In order to create coolant films for cooling surfaces, film cooling necessitates expelling coolant air through internal cooling channels. The heat transfer between hot current flow and surfaces is prevented by these cooling layers [5].

To enhance film cooling effectiveness, a great deal of pertinent research has been done Throughout the previous many decades. The study on film cooling in various eras was summed up in turn by [6-9]. Hole configuration, turbine geometry, and mainstream/coolant conditions are the three primary elements influencing film cooling performance. Numerous sub-parameters, such as holes shapes, surface curvature, a mass-to-flow ratio, a ratio of momentum flux, intensity of turbulence, unsteadiness and rotation, can be added to these main factors. The interdependence of such sub-parameters raises the bar for reliable film cooling performance prediction. Essentially, the jet in crossflow (JICF) problem is embodied by film cooling.

High mainstream turbulence broadens the coolant and hot flow mixing process after the cooling jet, leading to a small jet footprint. However, powerful mainstream turbulent flow more severely disturbs the near wall vortex. The efficiency and ratio of heat flow are seldom affected by the vortex, which disappears quickly [10]. It is a (JICF) a problem by nature for film cooling to occur.

Many experimental studies [11-14] and numerical simulations [15,16] conducted to examine the flow characteristics of the JICF. Impact of vortexgenerator location on cooling efficacy have been investigated through numerical modeling. The vortexgenerators are positioned either before the film cooling hole, downstream, or upstream. Based on the results, vortexgenerator situated above a circular film cooling opening will perform better. [17]. The JICF has complicated flow patterns that include wake vortices downstream of the jet, horseshoe-shaped vortices around the jet's base (see Fig. 1), shear-layer vortices in jets surrounding the jet's perimeter, and a counter-rotating vortex pair (CRVP) within the jet. Vortex that has the greatest bearing on film cooling effectiveness is CRVP.

Nomenclature			
K	Turbulent kinetic energy	**Subscripts**	
U	Velocity	c	coolant
T	Temperature	h	hot
t	time	x	Local distance
X	coordinate of mainstream flow direction	int	inlet
S	Source terms		
S_{ij}	Strain rate tensor	**Abbreviations**	
E_0	Total internal energy	VG	Vortex generator
D_h	Hydraulic diameter of duct	CRVP	Counter rotating vortexgenerator
Greek symbols		ACRVP	Anti-counter rotating vortexgenerator
ρ	Density	CFD	computational fluid dynamics
ε	Dissipation rate	DWVG	Downwash vortexgenerator
η	Film cooling effectiveness	BR	Blowing ratio
μ	Dynamic viscosity		

The CRVP was discovered to encourage the jet's entrainment entering the primary flow, which lowers the effectiveness of cooling. Consequently, the main challenge with film cooling is to lessen negatives effect of CRVP. Reducing the momentum of the exit jet or producing an extra (ACRVP) have been two strategies to increase the effectiveness of film cooling. The prevailing strategies mostly utilize vortex generators (VGs), upstream ramps, pulsation modulating devices, curved film holes, shallow trench film holes, and plasma actuators. Zhang et al [8] examined these techniques.

Impact of plasma actuators on the cooling of films have been the focus of some research in last decades. [18,19] investigated the impact of film cooling using plasma actuation. Findings indicated that by positioning the actuator downstream of the cylindrical hole, plasma actuators enhanced cooling performance by improving flow adhesion and achieving a larger flow coverage range.

Cau et al [20] studied four different types of film holes—fan shaped, cylindrical, sister, and anti-vortexto examine how flow structure and the effectiveness are affected by hole shape and blowing ratio. According to the results, fan-shaped works best when blowing ratios are high.

[21] conducted research regarding how the film hole affects pressure side film cooling properties about trailing-edge reduction in gas turbine which be elevated pressure vanes. [22] investigated a double wall cooling arrangement featuring ribs that are fashioned like flowers rather than the more common cylindrical ribs. [23] conducted the impacts of different Mach number during the cooling of film in transonic crossflow.

Recent decades have seen a significant increase in interest in the use of vortexgenerators (VG), also known as upstream ramps, to regulate the cooling film flow. As a result of boundary layer separation, a backflow zone will be created when a fluid crosses a step, which these VG take advantage of. The main stream diverges upward. upon encountering a ramp, reducing its impact on the film jet, but the lateral diffusion of coolant is facilitated by the area with low pressure backflow situated beyond the ramp.

[24,25] investigated how to increase the film cooling process using vortexgenerators downstream. Zhang et al.'s experimental study [24-26] examined the impact of an upstream vortex generator's inclination angle, height, and position on the film cooling enhancement effect. When [27] built and contrasted the upwash vortexgenerator (UWVG) and a downwash vortexgenerator (DWVG) with varying height parameters, they found that whereas UWVG had the opposite effect, DWVG improved film cooling. [28] used different vortexgenerators both single- and two-phase flows to enhance heat convection coefficient. [29] also examined a transverse trench and a tetrahedral ramp combination.

Even while earlier research has already shown that the VG can create downwash vortices to improve the performance of film cooling, these studies often concentrate on just one kind of vortexgenerators (VG).

In this study, vortex generators in the upper location of the hole were investigated numerically. A numerical simulation by utilizing CFD with a Realizable k-ε turbulence model. The present investigation differs from earlier research in because of using a two various kinds of vortexgenerators to improve film cooling effectiveness.

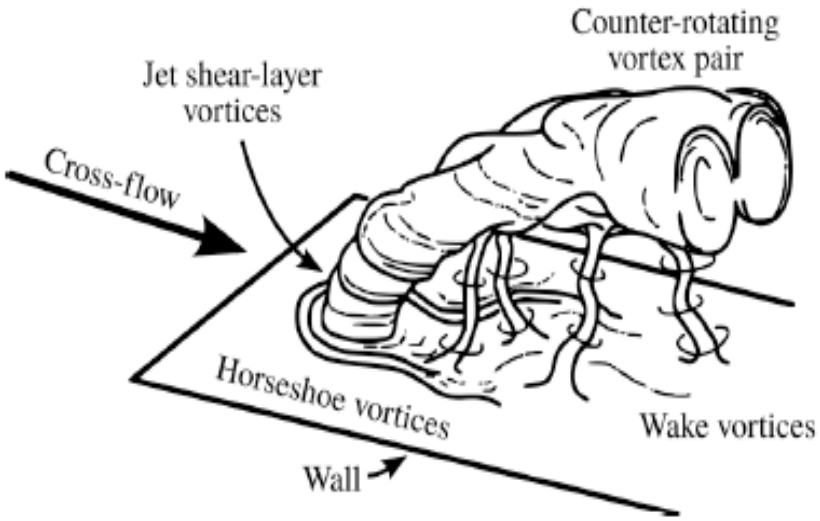

FIGURE 1. - Vortical structure in crossflow for the jet[30]

2. NUMERICAL SIMULATION

2.1 GEOMETRY

This paper's domain is a tube with a 7 mm diameter, inclined at a 30° angle. It also includes a duct for hot air, measuring 15 × 15 cm with a length of 122 cm. A box measuring 15 × 15 cm, was used to supply cold air. See Fig. 2.

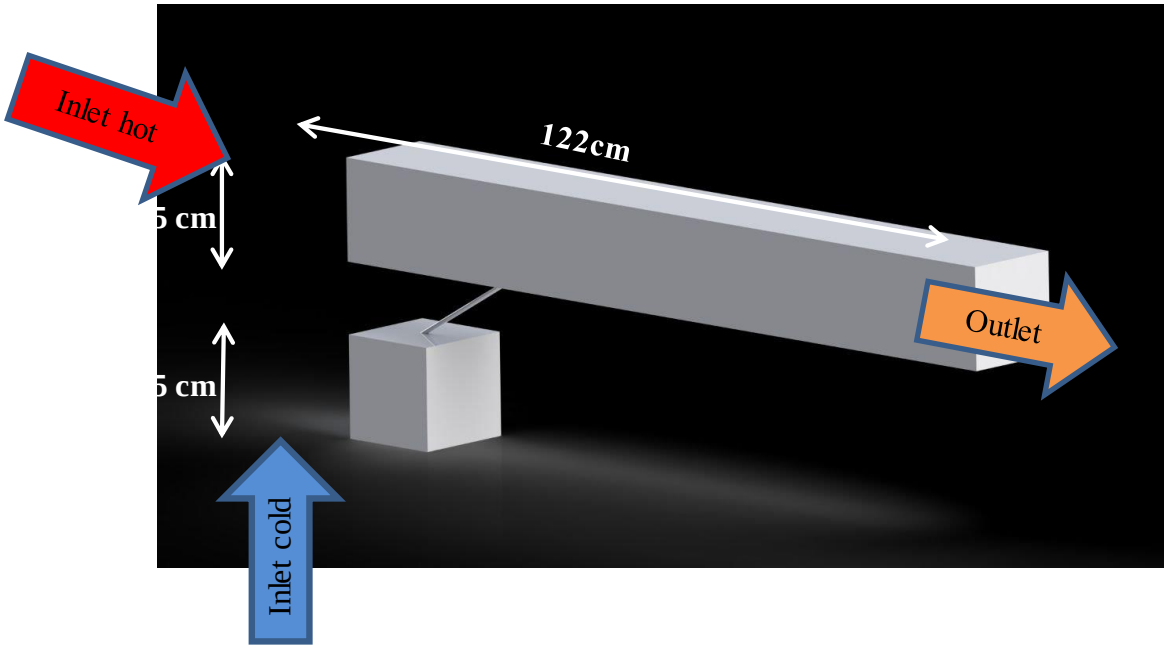

FIGURE 2. - Configuring Boundary Conditions

2.2 BOUNDARY CONDITIONS

The parameters for the boundary conditions employed in this study are displayed in Table 1.

Table 1.- Parameters for the boundary condition

Boundary condition	Value
Main flow temperature	348.15 (k)
Temperature of the jet flow	298.15 (k)
Blowing ratio	0.5, 1, 1.5, 2
Reynold number for air of the jet	3785 - 15150
Density ratio	1.2
Turbulent intensity of both coolant and mainstream	0.2%

2.3 VORTEX GENERATORS

In this research, two types of vortex generators were used:
a) A protrusion V-shaped vortex generator, with a height of 3.175mm, as depicted in Fig. 3.
b) A rectangular vortex generator, which used two rectangular vortex generators with dimensions of 4 × 8 mm, as shown in Fig. 4.

.

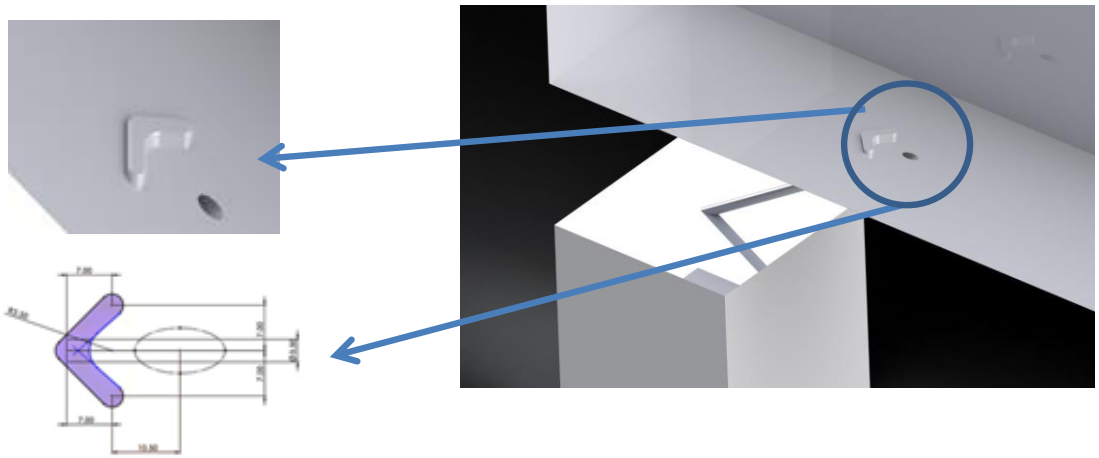

FIGURE 3. - The protrusion vortex generator

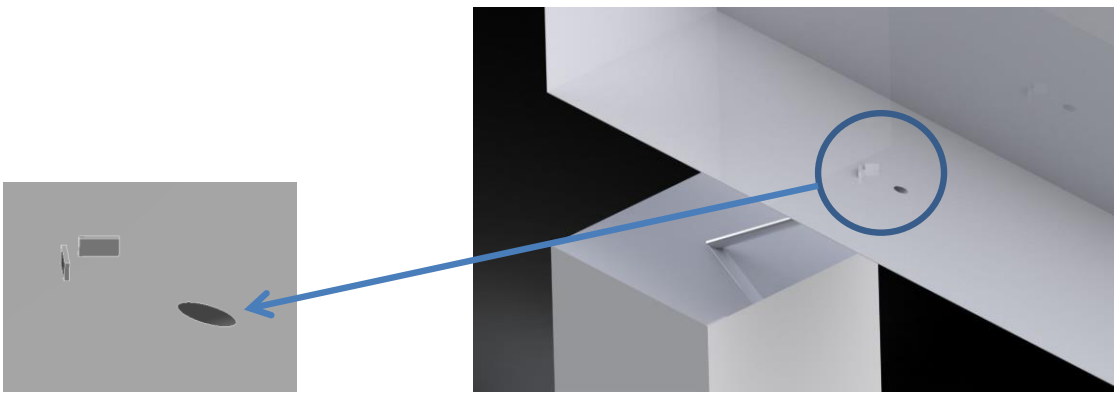

FIGURE 4. - Rectangular winglet pairs are vortex generators

2.4 VERIFICATIONS OF TURBULENCE MODEL AND MESH SIZE

To determine to which model of turbulence is capable of predicting cooling performance with accuracy, turbulence models are validated. Five turbulence models are considered, containing Realizable k-ε model, Standard k-ε model, RNG k-ε model, k- Omega, and Shear Stress Transport (SST), the effectiveness of film cooling is compared with the

experimental results of Zhou et al [31] under a blowing ratio of 0.5 and based on the baseline case. Trend and variable characteristics of the effectiveness of adiabatic film cooling in a streamwise direction can be accurately predicted by all turbulence models. When predicting the effectiveness of adiabatic cooling, the findings produced by the Realizable k-ε turbulence model in Fig. 5 correspond more closely to the experimental than do the outcomes from other turbulence models. So, Realizable k-ε model is utilized in current work.

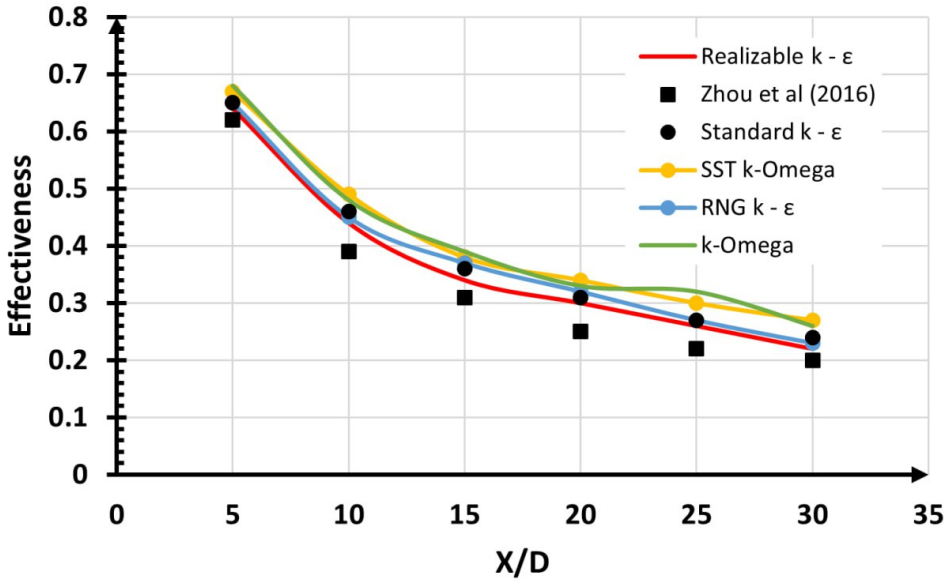

FIGURE 5. - Effectiveness of centerline adiabatic cooling at BR = 0.5 is compared between CFD findings and experiment data using various turbulence models

ANSYS Fluent 16.0 is used to produce meshes. The zones close to the wall and hole outlet are refined, and tetrahedron meshes partition the entire computational domain (see Fig. 6). For the near wall meshes, the y^+ is about equal to 1. Realizable k- ε turbulence model is used to analyze grid independence based on the baseline case at a blowing ratio of 0.5. In situations when there are three meshes, film cooling effectiveness across a flat plate is computed. Fig. 7 shows that, with an average inaccuracy of 0.15%, the cooling effectiveness curves for grid numbers 2.3 million and 2.60 million nearly overlap. The average discrepancy, however, between the 2.30 million and 1.9 million mesh findings is 1.3%. Thus, in the current investigation, a grid number of 2.30 million is used.

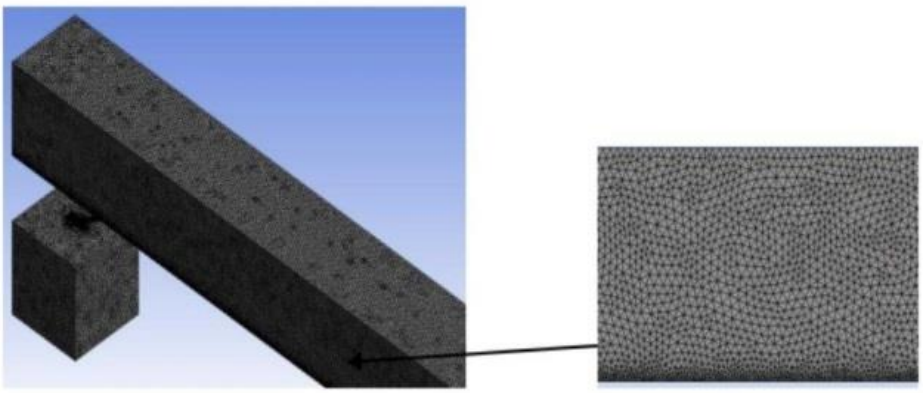

FIGURE 6. - Grids of the computational domain

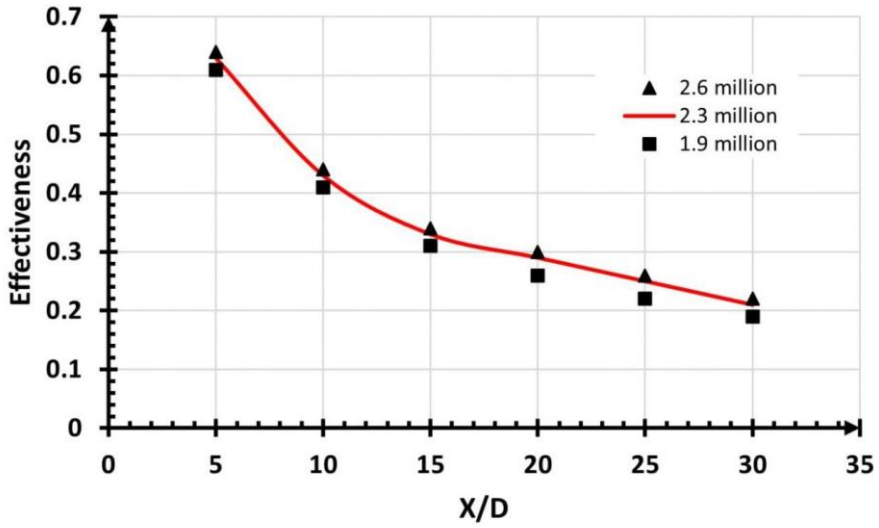

FIGURE 7. - Effectiveness of centerline adiabatic cooling with three mesh sizes is compared

2.5 GOVERNING EQUATION AND PARAMETERS DEFFINITION

In the present study, energy, momentum, and steady continuity equations in Cartesian coordinates are resolved to determine the heat transfer and flow characteristics.

The governing equations are [32]

Continuity equation is defined as:

$$\frac{\partial \rho}{\partial t}+\frac{\partial(\rho u_i)}{\partial x_i}=0 \quad (1)$$

Momentum equation is defined as:

$$\frac{\partial(\rho u_i)}{\partial t}+\frac{\partial(\rho u_i u_j)}{\partial x_j}=-\frac{\partial P}{\partial x_i}+\frac{\partial}{\partial x_j}(2\mu S_{ij})+\rho g_i+F_i \quad (2)$$

Where F_i the force of the body

S_{ij} is the tensor of strain rate

Energy equation is defined:

$$\frac{\partial(\rho E_0)}{\partial t}+\frac{\partial(\rho u_i u_j)}{\partial x_i}=\rho u_i F_i-\frac{\partial q_i}{\partial x_i}+\frac{\partial}{\partial x_j}(u_i T_{ij}) \quad (3)$$

Where E_0 is the total internal energy.

Furthermore, CFD was used to simulate this paper numerically at a steady state with the Realizable k-Ɛ turbulence model. At a steady state, solve energy and momentum equations. The coupled method and second-order wind were used. The density of the material was used for an incompressible ideal gas.

These transport equations yield the turbulent kinetic energy, k, and its dissipation rate, ε:

$$\frac{\partial}{\partial t}(\rho k)+\frac{\partial}{\partial x_j}(\rho k u_j)=\frac{\partial}{vx_j}\left[(\mu+\frac{\mu_t}{\sigma_k})\frac{\partial k}{\partial x_j}\right]+G_k+G_b-\rho\varepsilon-Y_M+S_k \quad (4)$$

$$\frac{\partial}{\partial t}(\rho\varepsilon)+\frac{\partial}{\partial x_j}(\rho\varepsilon u_j)=\frac{\partial}{\partial x_j}\left[\left(\mu+\frac{\mu_t}{\sigma_\varepsilon}\right)\frac{\partial\varepsilon}{\partial x_j}\right]+\rho C_1 S\varepsilon-\rho C_2\frac{\varepsilon^2}{k+\sqrt{v\varepsilon}}$$
$$+C_{1\varepsilon}\frac{\varepsilon}{k}C_{3\varepsilon}G_B+S_\varepsilon \quad (5)$$

Where C_1 max[0.43,$\frac{y}{y+5}$], $y=S\frac{k}{\varepsilon}$, $S=\sqrt{2S_{ij}S_{ij}}$.

C_2 and $C_{1\varepsilon}$ are constant 1.9 and 1.44 respectively.

σ_k and σ_ε are the turbulent Prandtl numbers for k and ε, 1.0 and 1.2 respectively.

G_b reflects the creation of turbulence kinetic energy because of the gradient in mean velocity and buoyancy, in that order, and Y_M denotes the part that variable dilatation plays in the total dissipation rate of compressible turbulence. The user-defined source words are S_k and $S\varepsilon$

Blowing ratio is described as: $BR = \frac{\rho_c U_c}{\rho_h U_h}$ (6)

In Fig. 8, we put the plate's convective boundary condition at time t > 0, assuming that heat conduction is exclusively in the x-direction. This depicts the brief flow across a flat plate that has a uniform temperature of T_i initially. As shown in Figure 6, an energy balance on the plate can be calculated.

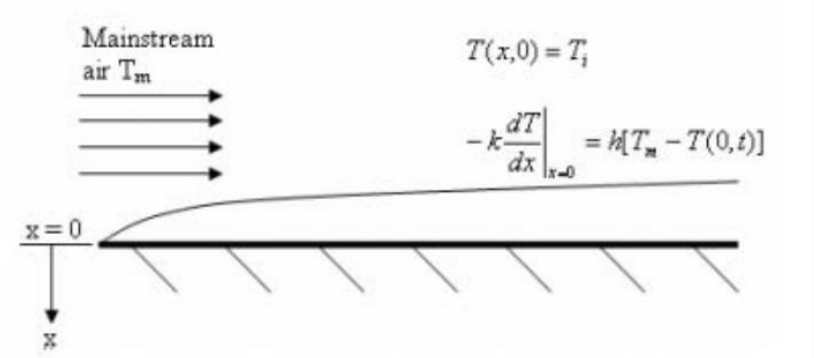

FIGURE 8. - Flow over flat plate [33]

Effectiveness is defined as:

$\eta = \frac{T_m - T_w}{T_m - T_c}$ (7)

2.6 VALIDATIONS

For validation purposes, the cooling effectiveness (η) for a conventional film cooling hole is plotted versus the axial distance X/D in Fig. 9. The current results at a blowing ratio of 0.5 and a hole angle of 30° are compared, for validation purposes, with the numerical result of Sarkar et al [27] and experimental work of Zhou et al [31] in this figure. With a maximum variance between experimental and numerical of roughly 3.5%, there was excellent agreement.

As per Ghorab's [34] earlier research, a maximum variation of ±10% was indicated, meaning that this variance falls within the permitted range.

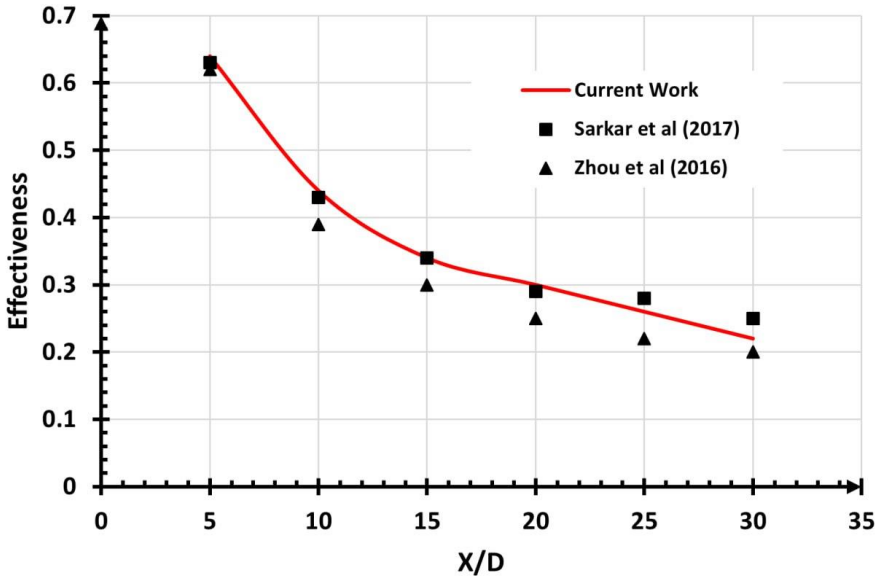

FIGURE 9. - Validation with previous studies at BR = 0.5 and β = 30°

3. RESULTS AND DISCUSSION

3.1 ANALYSIS OF FLOW CHARACTERISTICS

Upper perspective of the main stream when BR=0.5 for several examples is displayed in Fig. 10. Referencing Fig. 10 (a). as a model, The main mechanism of CRVP and a factor that hinders film cooling, the "entrainment effect," is readily noticeable in the baseline condition. It suggests that shear boundary between the film jet and the main flow causes the mainstream to shift along the lateral direction, inward.

The protrusion vortex generator is placed at the higher place of the hole, as shown in Fig. 10 (b). There is a zone of acceleration directly above the protrusion vortex generator due to a sharp drop in flow area, and the generator's leading edge has a zone of stagnant flow. when the mainstream contacts it. Moreover, the mainline forms tangled duos and extends outward to each side as it crosses the highest point of the protrusion vortex generator, rotating in the opposite direction from the CRVP.

A zone of low velocity exists behind VG in Fig. 10 (c) when rectangular vortex generator is used. VG area determines its size and shape, as it significantly affects the form drag on the region that faces the majority. A larger region could result in a greater low-speed region. Two zones of recirculating flow are observed behind the VG. Additionally, the interior recirculating zone is larger than the exterior due to the angle of attack. The pressure differential that exists as the mainline passes through VG is what creates the swirl flow. In this example, the swirl flow is more pronounced at the greatest region. Eventually, the downstream swirl flow becomes less strong.

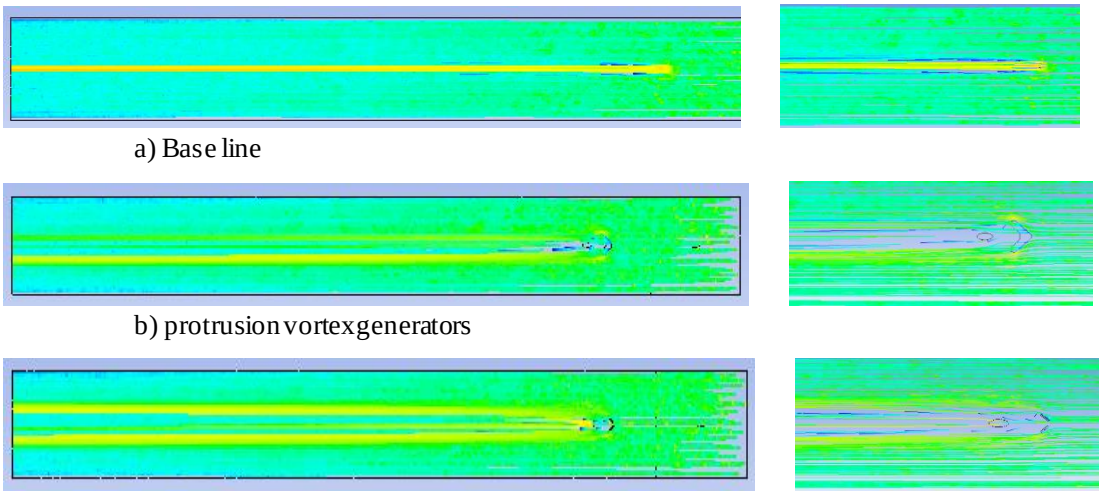

a) Base line

b) protrusion vortex generators

c) The rectangular vortex generator

FIGURE 10. - the top view of mainstream streamlines

3.2 FILM COOLING EFFECTIVENESS

Fig. 11, displays the temperature contour in the Y-Z section for $X/D_h = 5$ at BR = 0.5, 1, 1.5, and 2. Findings reveal that the CRVP's core center height rises in tandem with BR. Jet momentum growing with increasing BR gives the jet has a greater potential to pierce it and blend in with the mainstream with more intensity, which explains the previously indicated behavior. Two extra ACRVP are found for both types of vortex generators, located on opposing sides of the CRVP, when the vortex generator cases at the same BR are compared to the baseline case. With its opposite orientation to that of the CRVP, the ACRVP may effectively reduce jet-off and enhance coolant coverage laterally, hence enhancing film cooling effectiveness both spanwise and streamwise.

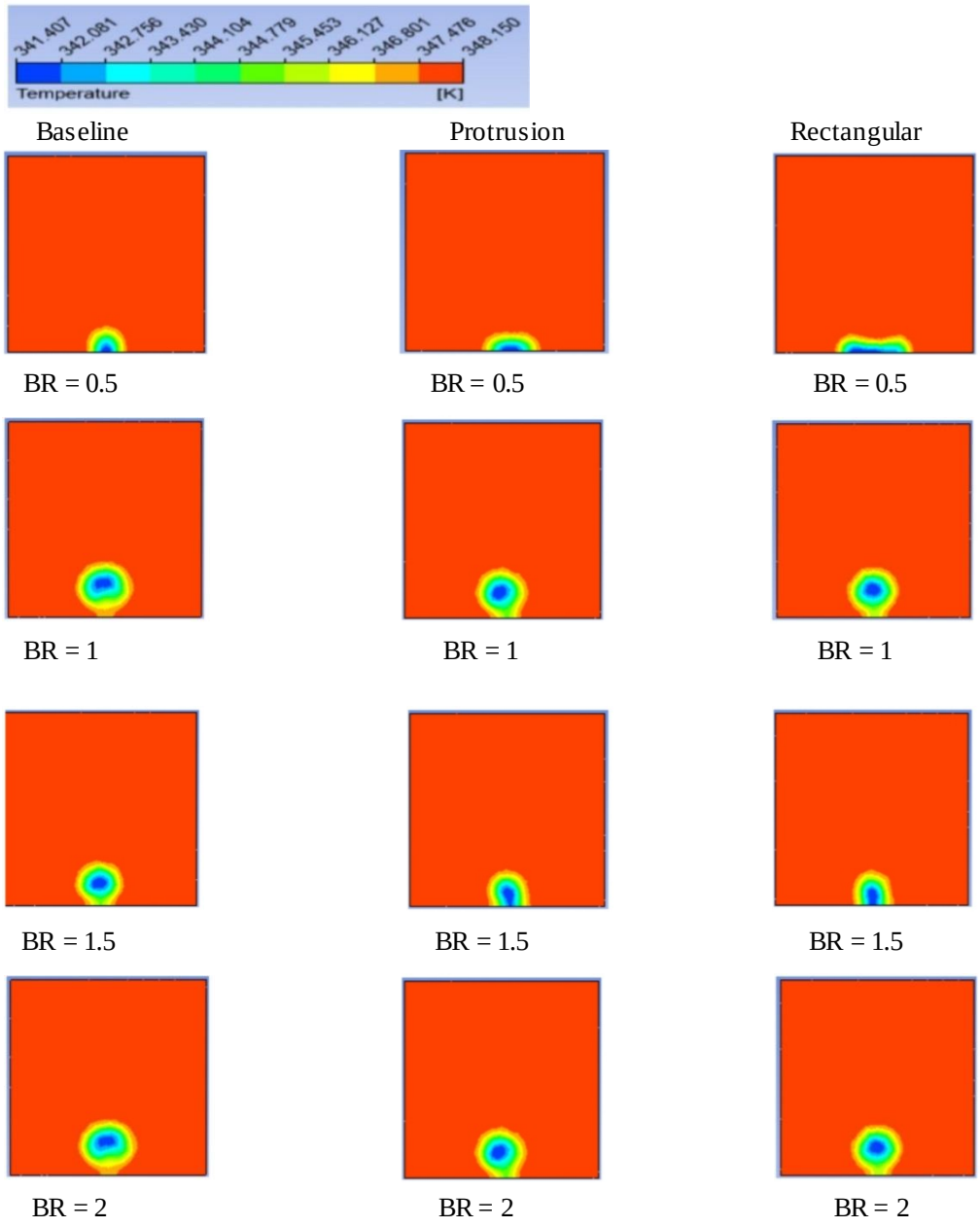

FIGURE 11. - A contour of temperature for X/D_h = 5 in the Y-Z section

Fig. 12, displays the temperature profile for a flat plate at various blowing ratios. This illustrates the usage of upstream vortex generators to improve film cooling efficiency. This makes sense: two additional ACRVP are created as vortex generators raise the mainstream, preventing CRVP from growing and the jet-off. Consequently, the center high cooling efficacy zone and lateral coverage have greatly expanded.

The distribution of temperature contour is depicted in Fig. 12. There is a clear indication that a layer of chilly air coated the flat plate's surface. The temperature of this cool air layer rises and gets cooler in the downstream direction of the hole of the jet. When the ratio of blowing was BR=0.5, the film jet's weak penetration into the main stream resulted in a longer air film-cooling layer covering one side of the surface than the other. Furthermore, the primary hot flow causes the film jet's flow direction to be curved toward the plate surface. In the meantime, as the figures below illustrate, the area covered by air film-cooling decreases at blowing ratios of 1.0, 1.5 and 2.0. Vortex effects and film cooling are combined in the vortex generators design. After going through a vortex generator, the main flow emerges onto the exterior of the flat plate. When the ratio of blowing was BR = 0.5, the film jet's weak penetration into the main stream resulted in a thicker air film-cooling layer covering the surface compared to the others. Furthermore, the primary hot flow causes the film jet's flow direction to be curved toward the plate surface. Concurrently, as illustrated in the following figures, the area covered by air film-cooling decreases at blowing ratios of 1.5, and 2.0.

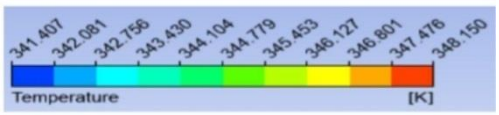

BR = 0.5

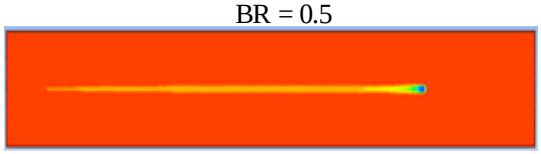

BR = 1

BR = 1.5

BR = 2

a) Baseline

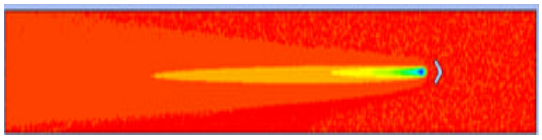

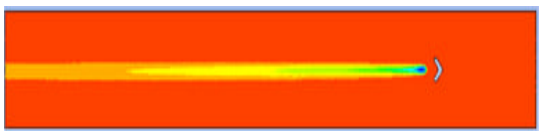

BR = 2

b) Protrusion vortexgenerator

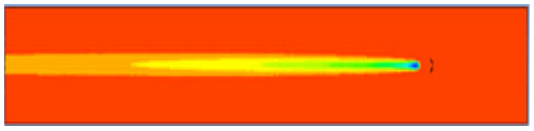

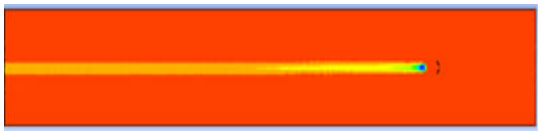

BR = 2

c) Rectangular vortexgenerators

FIGURE 12. - Contour of temperature for flat plate

Three instances of the plate surface temperature distribution are shown in Fig. 13. These numbers show that effectiveness decreases as blowing ratios rise over 1.0 because the cooling air jet blows far at high blowing ratios from the surface of plate, penetrating the hot stream.

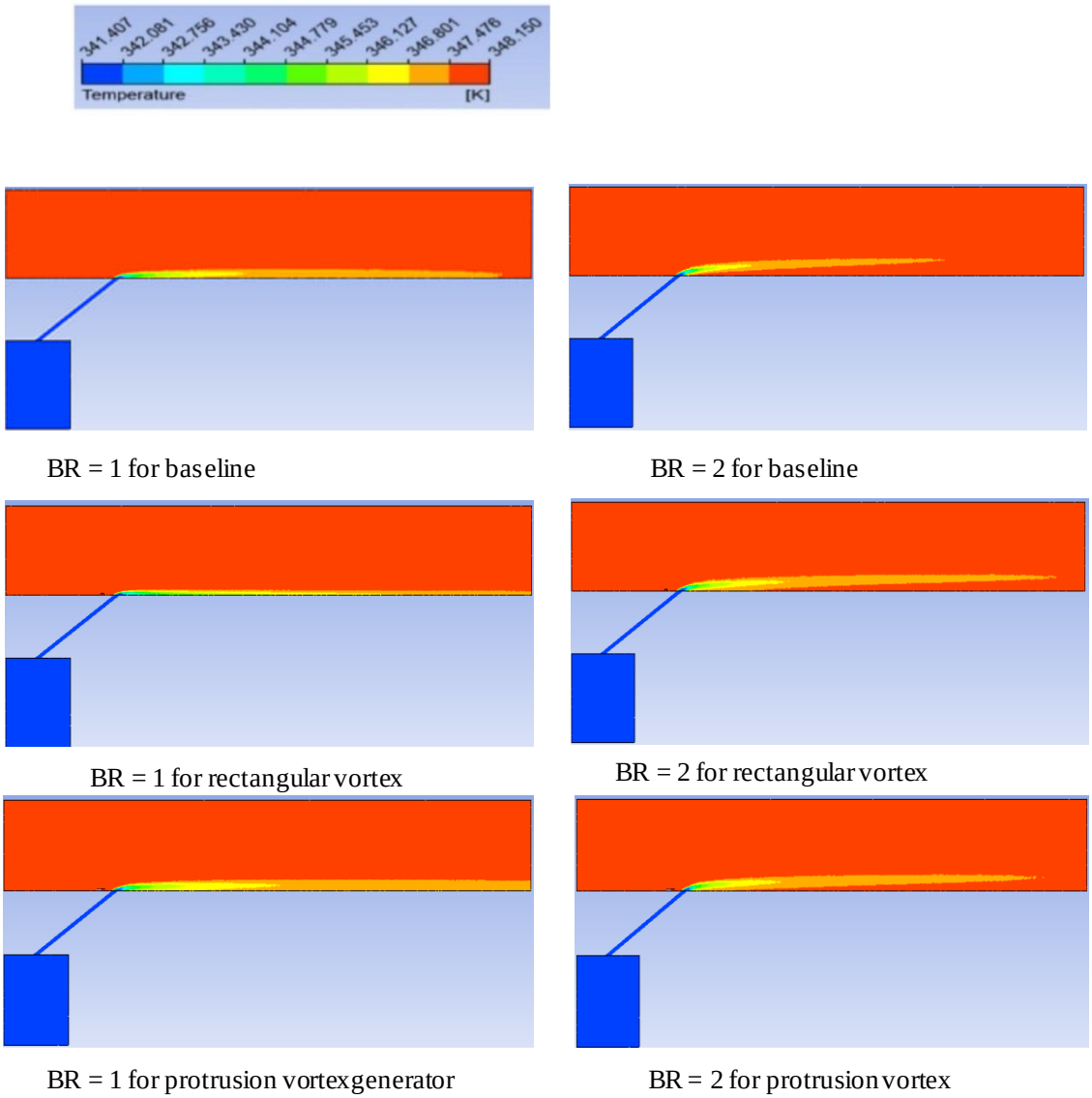

FIGURE 13. -The contours of temperature for the middle plane

Fig. 14, demonstrates that the 30-degree secondary coolant hole inclination provides the highest cooling effectiveness of each instance with a BR of 0.5, and with BR of 1, 1.5, and 2, it provides least protection. The highest effectiveness was reached when X/D = 5 at a blowing ratio of 0.5.

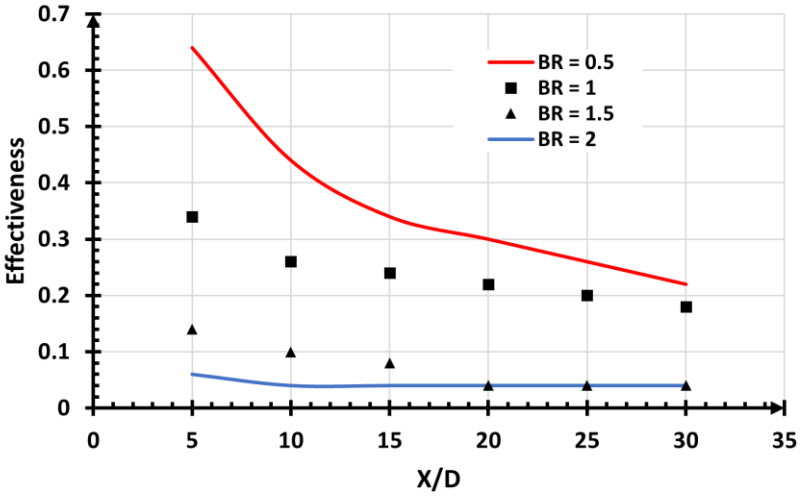

FIGURE 14. - **Effectiveness vs. streamwise location**

Film cooling performance of both types of vortex generators is increased upon raising the ratio of blowing from 0.5 to 1, as seen in Fig. 15 and Fig. 16.

The secondary flow and primary flow produce opposing vortexes to the additional ones that are developed. This increases the effectiveness of film cooling by forcing the cooling flow to adhere to the flat plate. The optimal efficiency was achieved with both types of vortex generators when the blowing ratio was equal to 1. Additionally, a rectangular vortex generator is more effective than a protrusion vortex generator (see Fig. 17) because it strongly suppresses the CRVP. Upon the BR increases to more than 1, effectiveness will decrease. This is because of the high flow rate of the coolant. As a result, Additional vortices cannot force the coolant to adhere to the flat plate properly.

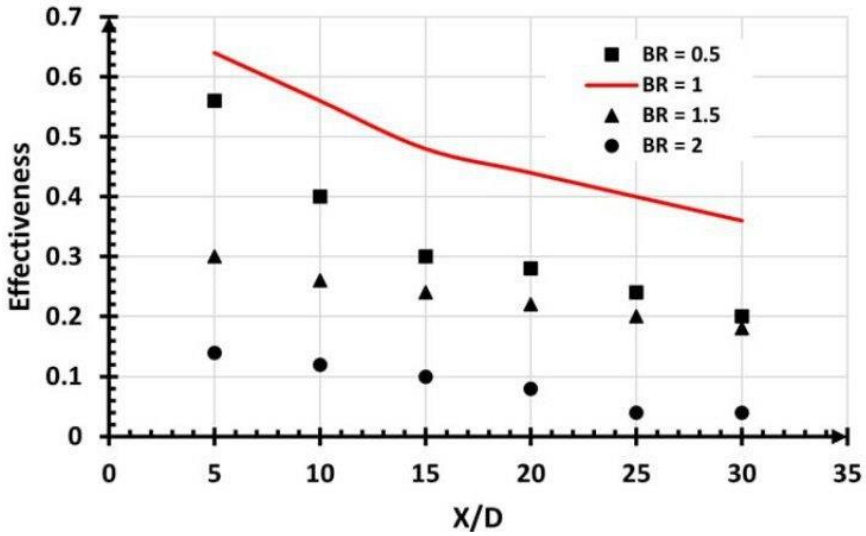

FIGURE 15. - **The protrusion vortex generator**

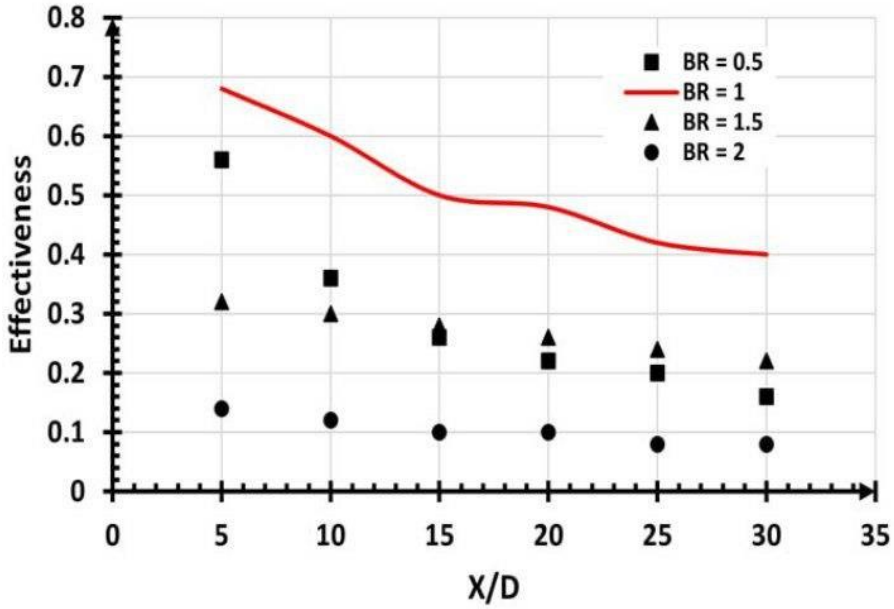

FIGURE 16. - The rectangular vortex generators

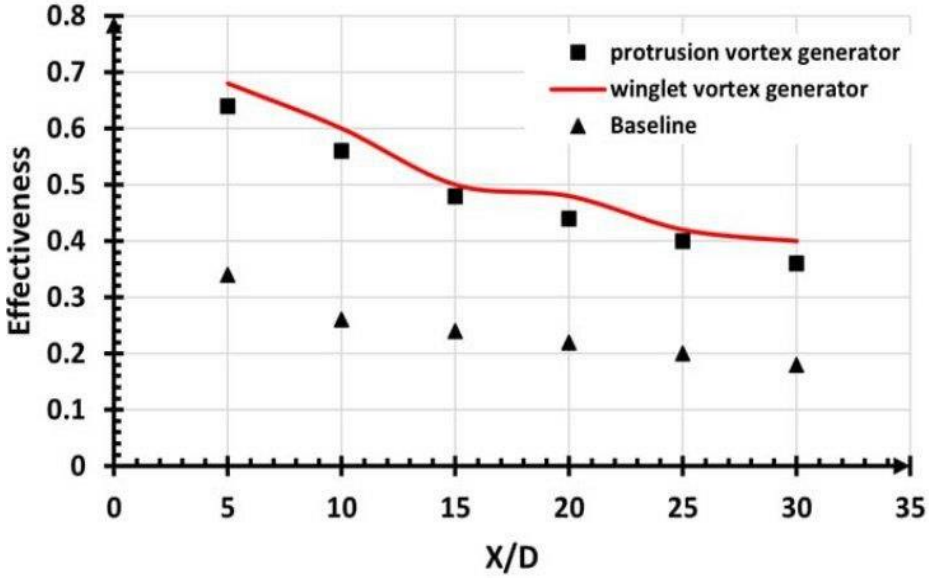

FIGURE 17. - Film cooling performance for a flat plate at BR = 1

4. CONCLUSION

To improve a flat plate's cooling effectiveness, vortex generators were employed. A numerical investigation is conducted on four blowing ratios utilizing vortex generators at the upper site of the cylindrical film hole. An overview of the main findings is provided below:

- When the blowing ratio was increased, the case without a vortex generator demonstrated less effective film cooling. The aforementioned behavior can be elucidated by the reality that jet's momentum increases as BR increases, strengthening the jet's ability to enter the main stream and increasing its density to mix with it outside of the flat plate.
- Vortex generators work to form additional anti-vortex generators to reduce the effect of CRVP.
- For both kinds of vortex generators, increasing the BR from 0.5 to 1, increases film cooling coverage and the effectiveness of film cooling. The secondary flow and a main flow produce opposing vortexes to the additional ones that are developed. This rises the effectiveness of film cooling by forcing the cooling flow to adhere to the flat plate.
- The highest efficiency was obtained when using a blowing ratio equal to 1.0 for both types of vortex generators.

- At the blowing ratio of 1.0, the greatest increase in the efficiency of film cooling for protrusion and rectangular vortex generators compared with a Baseline case are 24% and 27.33%, respectively.
- As the blowing ratio rises to more than 1, most of the coolant escapes away from the flat plate, resulting in a decrease in downstream film cooling effectiveness. This is because of the high flow rate of the secondary flow. As a result, Additional vortices cannot force the coolant to adhere to the flat plate properly

FUNDING

None

ACKNOWLEDGEMENT

The authors would like to thank the anonymous reviewers for their efforts.

CONFLICTS OF INTEREST

The authors declare no conflict of interest

REFERENCES

[1] M. A. Alvin, K. Klotz, B. McMordie, D. Zhu, B. Gleeson, and B. Warnes, "Extreme temperature coatings for future gas turbine engines," J. Eng. Gas Turbines Power, vol. 136, no. 11, p. 112102, 2014.
[2] E. A. Ogiriki, Y. G. Li, and T. Nikolaidis, "Prediction and analysis of impact of thermal barrier coating oxidation on gas turbine creep life," J. Eng. Gas Turbines Power, vol. 138, no. 12, p. 121501, 2016.
[3] X. Chen, Y. Long, Y. Wang, S. Weng, and Y. Luan, "Large eddy simulation of film cooling from cylindrical holes partially blocked by CaO-MgO-Al2O3-SiO2," Int. Commun. Heat Mass Transf., vol. 129, p. 105754, 2021.
[4] W. Jin, Y. X. Jia, J. Lei, W. T. Ji, and J. M. Wu, "Coupled heat transfer analysis of internal and film cooling of turbine blade under medium temperature conditions," Appl. Therm. Eng., vol. 214, p. 118792, 2022.
[5] Z. H. U. Rui, S. Terrence, L. I. Shulei, and X. I. E. Gongnan, "Film cooling performance and flow structure of single-hole and double-holes with swirling jet," Chinese J. Aeronaut., vol. 35, no. 3, pp. 201–213, 2022.
[6] R. S. Bunker, "A review of shaped hole turbine film-cooling technology," J. Heat Transf., vol. 127, no. 4, pp. 441–453, 2005.
[7] D. G. Bogard and K. A. Thole, "Gas turbine film cooling," J. Propuls. power, vol. 22, no. 2, pp. 249–270, 2006.
[8] J. Zhang, S. Zhang, W. Chunhua, and T. A. N. Xiaoming, "Recent advances in film cooling enhancement: A review," Chinese J. Aeronaut., vol. 33, no. 4, pp. 1119–1136, 2020.
[9] R. Zhu, G. Zhang, S. Li, and G. Xie, "Combined-hole film cooling designs based on the construction of antikidney vortex structure: a review," J. Heat Transfer, vol. 143, no. 3, p. 30801, 2021.
[10] X. Cui, P. Liu, C. Lin, and R. Dai, "Freestream effects on the interaction between near-wall vortex and film ejected from a fan-shaped hole," Exp. Therm. Fluid Sci., vol. 139, p. 110721, 2022.
[11] R. M. Kelso, T. T. Lim, and A. E. Perry, "An experimental study of round jets in cross-flow," J. Fluid Mech., vol. 306, pp. 111–144, 1996.
[12] B. A. Haven and M. Kurosaka, "Kidney and anti-kidney vortices in crossflow jets," J. Fluid Mech., vol. 352, pp. 27–64, 1997.
[13] T. H. New, T. T. Lim, and S. C. Luo, "Elliptic jets in cross-flow," J. Fluid Mech., vol. 494, pp. 119–140, 2003.
[14] A. Sau, T. W. H. Sheu, S. F. Tsai, R. R. Hwang, and T. P. Chiang, "Structural development of vortical flows around a square jet in cross-flow," Proc. R. Soc. London. Ser. A Math. Phys. Eng. Sci., vol. 460, no. 2051, pp. 3339–3368, 2004.
[15] E. Sakai, T. Takahashi, and H. Watanabe, "Large-eddy simulation of an inclined round jet issuing into a crossflow," Int. J. Heat Mass Transf., vol. 69, pp. 300–311, 2014.
[16] C. Dai, L. Jia, J. Zhang, Z. Shu, and J. Mi, "On the flow structure of an inclined jet in crossflow at low velocity ratios," Int. J. Heat Fluid Flow, vol. 58, pp. 11–18, 2016.
[17] N. Halder, "Numerical Inspection of location, density ratio and turbulent kinetic energy of vortex generator in gas turbine blade film cooling application," J. Therm. Sci. Eng. Appl., pp. 1–22, 2024.
[18] J. Sun, F. Zhang, J. Wang, G. Xie, and B. Sundén, "Effects of plasma actuation and hole configuration on film cooling performance," Propuls. Power Res., vol. 12, no. 2, pp. 227–237, 2023.
[19] J. Sun, G. Xie, J. Wang, and B. Sunden, "Enhanced film cooling and flow disturbance of an AGTB turbine cascade with plasma aerodynamic actuation at film-holes outlets," Int. Commun. Heat Mass Transf., vol. 140, p. 106522, 2023.

[20] X. L. Nan Cao, Xue Li, "Effect of film hole geometry and blowing ratio on film cooling performance," Appl. Therm. Eng., vol. 165, p. 114578, 2020.
[21] P. Wang, Q. Xu, J. Liu, P. Wang, Q. Du, and Z. Wang, "Experimental and unsteady numerical investigations on cooling characteristics of trailing-edge cutback with effect of upstream film holes," Int. J. Therm. Sci., vol. 193, p. 108423, 2023.
[22] Y. Luan, L. Zhang, L. Yang, Y. Yin, F. Magagnato, and T. Sun, "Research for double wall cooling configuration with flower shaped ribs," Int. J. Therm. Sci., vol. 193, p. 108493, 2023.
[23] H. Guo, P. Jiang, W. Peng, and Y. Zhu, "Large eddy simulation of highly compressible film cooling in transonic crossflow," Int. J. Heat Mass Transf., vol. 202, p. 123765, 2023.
[24] L. Song, C. Zhang, Y. Song, J. Li, and Z. Feng, "Experimental investigations on the effects of inclination angle and blowing ratio on the flat-plate film cooling enhancement using the vortex generator downstream," Appl. Therm. Eng., vol. 119, pp. 573–584, 2017.
[25] D. Straub, J. Weber, A. Roy, C.-S. Lee, and T. I. P. Shih, "Effects of Downstream Vortex Generators on Film Cooling a Flat Plate Fed by Crossflow," J. Turbomach., vol. 146, no. 5, 2024.
[26] C. Zhang, J. Wang, X. Luo, L. Song, J. Li, and Z. Feng, "Experimentally measured effects of height and location of the vortex generator on flow and heat transfer characteristics of the flat-plate film cooling," Int. J. Heat Mass Transf., vol. 141, pp. 995–1008, 2019.
[27] S. Sarkar and G. Ranakoti, "Effect of vortex generators on film cooling effectiveness," J. Turbomach., vol. 139, no. 6, p. 61009, 2017.
[28] A. Q. Ibrahim and R. S. Alturaihi, "Experimental work for single-phase and two-phase flow in duct banks with vortex generators," Results Eng., vol. 15, p. 100497, 2022.
[29] B. Kröss and M. Pfitzner, "Numerical and experimental investigation of the film cooling effectiveness and temperature fields behind a novel trench configuration at high blowing ratio," in Turbo Expo: Power for Land, Sea, and Air, American Society of Mechanical Engineers, 2012, pp. 1197–1208.
[30] T. F. Fric and A. Roshko, "Vortical structure in the wake of a transverse jet," J. Fluid Mech., vol. 279, pp. 1–47, 1994.
[31] W. Zhou and H. Hu, "Improvements of film cooling effectiveness by using Barchan dune shaped ramps," Int. J. Heat Mass Transf., vol. 103, pp. 443–456, 2016.
[32] J. He, Q. Deng, and Z. Feng, "Film cooling performance enhancement by upstream V-shaped protrusion/dimple vortex generator," Int. J. Heat Mass Transf., vol. 180, p. 121784, 2021.
[33] A. F. Abdulwahid, T. M. Lazim, A. Saat, and Z. S. Kareem, "Investigation of Effect Holes Twisted Angle and Compound Angle of Holes on Film Cooling Effectiveness," Int. Rev. Autom. Control, vol. 8, no. 3, pp. 244–250, 2015.
[34] M. G. Ghorab, "Experimental investigation of advanced film cooling schemes for a gas turbine blade." Concordia University, 2009.